Nuclear import of factors involved in signaling is inhibited in C3H/10T1/2 cells treated with tetradecylthioacetic acid

Bodil Bjørndal,[1,*] Charlotte Helleland,[*] Stig-Ove Bøe,[†] Oddrun A. Gudbrandsen,[§] Karl-Henning Kalland,[†] Pavol Bohov,[§,] Rolf K. Berge,[§] and Johan R. Lillehaug[*]**

Department of Molecular Biology,* University of Bergen, 5020 Bergen, Norway; Department of Microbiology and Immunology,† University of Bergen, Norway; Department of Clinical Biochemistry,§ University of Bergen, Norway; and Institute of Experimental Endocrinology,** Slovak Academy of Sciences, Bratislava, Slovak Republic

Abstract The non-β-oxidisable tetradecylthioacetic acid (TTA) is incorporated into cellular membranes when C3H/10T1/2 cells are cultured in TTA-containing medium. We here demonstrate that this alteration in cellular membranes affect the nuclear translocation of proteins involved in signal transduction. Analysis of cellular fatty acid composition shows that TTA and TTA:1n-8 constitute approximately 40 mol% of total fatty acids in cellular/nuclear membranes. Activation of c-*fos* expression is significantly inhibited in TTA-treated cells but the enzymatic activation of mitogen activated protein kinase (ERK) is not affected. Immunofluorescence and confocal microscopy studies demonstrate that in mitogene-stimulated TTA-treated cells, the translocation of phosphorylated ERK1/2, protein kinase Cα (PKCα), and PKCβ$_1$ from the cytoplasm into the nucleus is considerably decreased and delayed. Concomitant with a decreased nuclear import, ERK1/2 dephosphorylation is decreased in TTA-treated cells. There is no TTA-induced inhibition of nuclear import of proteins with a classical nuclear localization signal (NLS), as seen by in vitro nuclear import experiments of BSA fused to the NLS from SV40 large T, or in vivo studies of hnRNP A1 nuclear import. The expression levels of Importin α, Importin β, Importin 7, and NTF2 are not altered in the TTA-treated cells. Taken together, our data indicate that TTA treatment causes changes in cellular fatty acid composition that negatively affect NLS-independent mechanisms of protein translocation through the nuclear pore complex.—Bjørndal, B., C. Helleland, S-O. Bøe, O. A. Gudbrandsen, K-H. Kalland, P. Bohov, R. K. Berge, and J. R. Lillehaug. **Nuclear import of factors involved in signaling is inhibited in C3H/10T1/2 cells treated with tetradecylthioacetic acid. *J. Lipid Res.* 2002.** 43: **1630–1640.**

Supplementary key words TTA • mitogen-activated protein/extracellular signal-regulated kinase • protein kinase C • nuclear translocation

We have investigated the metabolic effects of a novel sulfur-substituted fatty acid analog, tetradecylthioacetic acid [CH_3-$(CH_2)_{13}$-S-CH_2COOH] (TTA), that has major impact on cellular metabolism (1, 2). TTA has many chemical and physical properties in common with normal saturated fatty acids, but it cannot undergo β-oxidation (1). When administered to rats, TTA promotes hepatic peroxisome and mitochondria proliferation and decreases serum triacylglycerol, cholesterol, and free fatty acid levels (3–5). TTA is known to affect the expression and activity of several genes involved in lipid metabolism (5–11), and is incorporated into liver lipids and plasma lipoproteins. We have previously found that TTA increases the formation of phosphatidylethanolamine (PE) with a shift from less to more polar molecular species in fibroblasts, and that TTA attenuates PDGF- and 12-*O*-tetradecanoyl phorbol-13-acetate (TPA)-induced c-*fos* mRNA expression (12). Altogether, TTA seems to alter the lipid composition in the cells in a manner that effects the PDGF- and TPA-induced signal transduction pathway leading to the regulation of c-*fos* mRNA expression.

The mitogen-activated protein kinase (MAPK) cascades are essential for signaling of various extracellular stimuli to the nucleus, and the Ras-mitogen-activated protein/extracellular signal-regulated kinase kinase (MEK)-mitogen-activated protein/extracellular signal-regulated kinase (ERK) pathway is important in regulating c-*fos* transcription. The triggering step in this pathway is the translocation of ERK1 and ERK2, also known as p44 and p42 MAPK, respectively, from the cytoplasm to the nucleus (13–15), where they activate nuclear factors such as Elk-1 by phosphorylation (16). Activation and nuclear translo-

Manuscript received 28 November 2001, in revised form 19 April 2002, and in re-revised form 27 June 2002.

DOI 10.1194/jlr.M100406-JLR200

Abbreviations: DAG, diacylglycerol; ERK, mitogen-activated protein/extracellular signal-regulated kinase; MAP, mitogen-activated protein; MBP, myelin basic protein; MEK, mitogen-activated protein/extracellular signal-regulated kinase kinase; NLS, nuclear localization signal; NPC, nuclear pore complex; PDGF-BB, platelet-derived growth factor-BB; PE, phosphatidylethanolamine; PKC, protein kinase C; TPA, 12-*O*-tetradecanoyl phorbol-13-acetate; TTA, tetradecylthioacetic acid.

[1] To whom correspondence should be addressed.
e-mail: bodil.bjorndal@mbi.uib.no

cation of ERK1/2 is required for mitogen-induced gene expression and cell cycle re-entry (17), making nuclear translocation a critical step in signal transduction. Unphosphorylated ERK is believed to be retained in the cytoplasm by complexing with proteins such as MEK (MAPK kinase) (18) and protein thyrosine phosphatase PTP-SL (19). The phosphorylation of ERK by MEK results in the dissociation of the ERK-MEK complex (18). The subsequent import mechanism has been most extensively studied for ERK2; three mechanisms have been identified: passive diffusion of a monomer, active transport of a phosphorylated ERK2 dimer (20, 21), or a recently discovered third pathway where ERK can be imported into the nucleus by direct contact with the nuclear pore complex (NPC) independent of phosphorylation, energy, or transport factors (22, 23). However, the exact mechanism by which ERK1/2 passes through nuclear pores has not been fully elucidated, and ERK does not contain a classical nuclear localization signal (NLS). Taken together, ERK enzyme activation and nuclear translocation are separable events (24). Stimulating the cells with TPA or platelet-derived growth factor-BB (PDGF-BB) showed that the ERK activity was the same in both control and TTA-treated cells. These results indicated that the pathway(s) activating ERK was not altered by the 3-thia fatty acid. Indirect immunofluorescence of total ERK1/2 and activated pERK1/2 showed, however, that the translocation of pERK1/2 from cytoplasm to the nucleus was significantly reduced in TTA-treated cells.

Recently, we have demonstrated that protein kinase Cα (PKCα) and PKCβ_1 in C3H/10T1/2 cells are translocated from the cytoplasm to the nucleus in response to TPA stimulation, but not in response to PDGF-BB stimulation (25). In this study we showed that this nuclear translocation of PKCα and PKCβ_1 was reduced in TTA-treated cells compared with control cells. Thus, other PKs involved in signal transduction were affected by TTA, and the inhibition of nuclear import was not unique to ERK. To further investigate the mechanism of the TTA-inhibition, a classical, lysine-rich NLS from SV40 large T antigen was coupled to BSA-fluorescein (FITC) and used to study nuclear import in digitonin-permeabilized cells. Neither the import kinetics of BSA fused to this strong NLS, nor the in vivo import of the NLS (M9)-containing protein hnRNP A1 was detectably inhibited in TTA-treated cells. Our results suggest that nuclear import of proteins without a classical NLS is inhibited in TTA-treated cells while NLS-directed import is unaffected.

MATERIALS AND METHODS

Cell cultures

The mouse embryo fibroblasts C3H/10T1/2Cl 8 (10T1/2) have been described previously (26). TTA was synthesized as previously described (1). Cells were seeded in basal minimal Eagle's medium (BMEM; GIBCO BRL) supplemented as described (25). After 24 h, TTA (20 μM, final concentration) was added to the appropriate cell cultures, and an equal amount of acetone was added to the control cultures. After 48 h the medium was changed to UltraMem (Bio Whittaker, Inc., Walkersville, MD) supplemented with 2% FCS containing 20 μM TTA (final concentration)/acetone. By analysis, TTA comprised 54 mol% of total fatty acids in the growth medium. The medium was changed every second or third day until the cells had reached confluence. Cells to be used for indirect immunofluorescence assays were at confluence trypsinised and reseeded onto coverslips (Merch Eurolab, Darmstadt, Germany) at a concentration of 10,000 cells per well. The cells were then grown for 3 days in UltraMem medium containing TTA/acetone before they were stimulated and fixed for subsequent indirect immunofluorescence assays.

Materials and antibodies

TPA from Sigma Chemical Co. (St. Louis, MO) was dissolved in acetone. Porcine platelet-derived growth factor (PDGF-BB) and Actinomycin D was from Sigma. Leptomycin B was a generous gift from Dr. Barbara Wolff (Sandoz Research Institute, Vienna, Austria). Rabbit polyclonal antibodies against ERK1 (H-8), ERK2 (D-2), c-PKCα (C-20), and c-PKCβ_1 (C-16) were from Santa Cruz Biotechnologies (Santa Cruz, CA), and the monoclonal antibody to phospho-p44/42 MAPK (E10, pERK1/2) was from New England Biolabs, Inc. (Beverly, MA). Monoclonal anti-hnRNP A1 (4B10) was the generous gift of professor Gideon Dreyfuss (University of Pennsylvania School of Medicine, Philadelphia, PA). FITC-conjugated goat-anti-rabbit IgG and goat-anti-mouse was from Southern Biotechnology Associates, Inc. (Birmingham, AL), and Alexa568-conjugated goat-anti-mouse was from Molecular Probes. Biotin-conjugated rabbit-anti-mouse and FITC-conjugated streptavidine were from Amersham Int. plc.

ERK activity determination

Cells were grown to confluence on 100 mm plastic culture dishes with final medium change 24 h prior to harvesting. Cells were stimulated with 1 unit of PDGF-BB for the appropriate time. 1 unit of PDGF-BB corresponds to the amount of stimulant giving half-maximal stimulation of DNA synthesis. Cells were washed three times with cold phosphate buffered saline (PBS) and lysed in 0.5 ml non-ionic detergent buffer (1% Triton X-100, 20 mM TrisHCl, pH 8.0, 137 mM NaCl, 10% glycerol, 2 mM EDTA, 1 mM PMSF, 50 mM sodium fluoride and 1 mM sodium orthovanadate), by gentle rocking for 20 min at 4°C. To amounts of cell lysate corresponding to 100 μg total protein, MAPK antibody (anti-ERK1, 1:100, v/v) was added and incubated for 2 h at 4°C. Twenty microliters protein A/G PLUS agarose-conjugate (Santa Cruz) was added for the last 30 min. Immuno-complexes were collected by micro-centrifugation, and washed twice in non-ionic detergent buffer and once in TBS containing 5 mM benzamidine and 1 mM sodium orthovanadate. MAPK activity was determined by addition of 40 μl of kinase reaction mixture containing 30 mM TrisHCl, pH 8.0, 10 mM MgCl, 20 μM ATP, 1 mM DTT, 5 mM benzamidine, 10 μCi of [γ-^{32}P]ATP (specific activity 3,000 Ci/mmol, Amersham), and 6 μg myelin basic protein (MBP) (Upstate Biotechnology, NY). After 30 min incubation at 37°C, the reaction was stopped by adding 20 μl sample buffer and samples were subjected to SDS-PAGE. The gel was fixed in 10% acetic acid, 50% ethanol for 30 min and vacuum dried for 2 h at 80°C. The gel was subjected to phospho-imager analyses (Instant Imager, Packard Electronic Autoradiography/ Instant Imager Scanning) and exposed to X-Ray film.

Indirect immunofluorescence and immunoblot analysis

The cells used for immunofluorescence were grown on glass coverslips, treated with 10% FBS, TPA (1.7 μM), or PDGF-BB (1 unit), and washed once at 37°C with a cytoskeleton buffer (CB)

(137 mM NaCl, 5 mM KCl, 1.1 mM $Na_2HPO_4 \cdot 2H_2O$, 0.4 mM KH_2PO_4, 5.5 mM glucose, 4 mM $NaHCO_3$, MES, pH 6.1, 2 mM EGTA, and 2 mM $MgCl_2$). Cells were fixed for 20 min at room temperature with 3.7% formaldehyde in CB, washed three times 10 min in PBS and then permeabilised for 10 min in 0.1% TritonX-100 in PBS. Cells were then incubated for 30 min with blocking solution (1% BSA in PBS) before incubation with antibodies against ERK1 (1:1,000, v/v), ERK2 (1:500, v/v), pERK1/2 (1:500, v/v), hnRNP A1 (4B10, 1:2,000, v/v), PKCα, or PKCβ_1 (1:1,500, v/v) in 0.5% BSA in PBS. Finally, the cells were incubated for 30 min with the appropriate secondary antibodies. Confocal Laser Scanning Microscopy was carried out using the Leica TCS Confocal System attached to a Leica DM RXA microscope with a 40× oil immersion objective, and with Leica PowerScan software. The figures were created using Adobe photoshop version 5.5.

For immunoblot analysis, cells were grown to confluence on 100 mm plastic culture plates with final medium change 24 h prior to harvesting. The cells were incubated with TPA or 10% FBS for the appropriate time, washed three times in ice cold PBS and lysed in non-ionic detergent buffer (1% triton X-100, 20 mM TrisHCl, pH 8.0, 137 mM NaCl, 1% glycerol, 2 mM EDTA, 1 mM PMSF, 50 mM NaF, 1 mM $NaVO_3$). About 20 μg of protein from the different samples were separated on 10% SDS-PAGE gels and subsequently blotted onto nitrocellulose membranes. Membranes were blocked in 5% non-fat dry milk in Tris-buffered saline-Tween 20 (0.5%) and incubated with rabbit polyclonal antibodies against c-PKCα (1:500, v/v). Bound antibodies were visualized using HRP-conjugated anti-rabbit IgG followed by enhanced chemoluminiscence (ECL) detection.

Purification of cell membranes and nuclei and fatty acid determination

Cells were grown to confluence on 100 mm plastic culture dishes and washed twice in ice-cold PBS. The cells were scraped with a rubber policeman in homogenising buffer (10 mM Hepes, pH 7.4, 50 mM sucrose, 1 mM PMSF). Passing the cell suspension 20 times through a stainless steel cell homogeniser (EMBL, Heidelberg, Germany) disrupted the plasma membrane. The nuclear fraction was collected by centrifugation using an Eppendorf micro-centrifuge at 6,300 rpm for 5 min. The nuclear fraction was free of intact cells but contained remains of nuclear associated endoplasmatic reticulum. The post-nuclear supernatant was centrifuged at 105,000 *g* for 1 h at 4°C to pellet the membrane fraction. Lipids from cell membranes and nuclei were extracted with chloroform-methanol (27) and transesterified with 14% BF_3-methanol (28). After alkaline hydrolysis of methyl esters (29), cholesterol and non-saponifiable material were removed and free fatty acids were determined on GC 8,000 Top gas chromatograph (CE Instruments, Milano, Italy), equipped with a flame ionisation detector, programmable temperature of vaporisation injector and AS 800 autosampler using a SP 2,340 fused silica capillary column (60 m × 0.25 mm × 0.20 μm) (Supelco, Bellefonte, PA). Chromatographic conditions were similar as referred (30). Identification of chromatographic peaks was performed by means of known standards (Larodan Fine Chemicals, Malmø, Sweden) and confirmed by GC/MS analysis (GCQ, Finnigan MAT, Austin, TX). Quantification was made with ChromCard A/D 1.0 chromatography station (CE Instruments, Milano, Italy) based on heneicosanoic acid as an internal standard.

In vitro semi-intact cell free assay system

NLS-BSA-FITC conjugates were prepared according to Hassel et al. (31) using FITC from Molecular Probes, (Eugene, OR), peptides from Research Genetics (San Diego, CA), and BSA from Boehringer Mannheim. In order to prepare for the in vitro transport reaction, cells with or without TTA pre-treatment were seeded onto glass coverslips and grown for 24 h. Cells were then washed once in PBS and once in ice-cold buffer T (20 mM HEPES pH 7.4, 110 mM KAc, 2 mM $MgCl_2$, and 0.5 mM EDTA). Permeabilization of cells was then carried out on ice for 7 min in the presence of buffer T containing 40 μg/ml digitonin (Sigma). Following an additional wash in buffer T, coverslips were inverted onto 25 μl reaction mixture consisting of 1.1 mM ATP, BSA-NLS-FITC (between 0.2 and 1.0 μM), and reticulocyte lysate (Promega, Madison, WI), 1:4, v/v. In control reactions, the reticulocyte lysate was replaced with buffer T. The reactions were performed for 5 to 30 min in a humidified chamber at 37°C and then terminated by fixation in 3.7% formaldehyde in PBS. Finally, cells were washed in PBS and mounted on slides.

Dot blot analysis

Dot blot was performed as described in Fluge et al. (32). PCR products were amplified from cDNA from 10T1/2-cells using specific primers (Eurogentec, Seraing, Belgium) for Importin α (F-TGATGATGCTACTTCTCCGCTACA, R-ATTGTGGTGCAGGAGTCGAACTA), Importin β (F-AGCAGAGGTGGCTCGCTATTG, R-AAGGGTTCCAGTCATCGTCGT), Importin 7 (F-GATAACACAATATTGGCCTGATCGG, R-GGCGCCATATATTGTTTTTCCTTGTAC), Nuclear Transport Factor 2 (NTF2, F-CCAGGATGGGAGACAAGCCAA, R-GAAGTTGTGCAGGGCAAGC), and Actin (F-GGCACCACACCTTCTACA, R-AGGAAGGCTGGAAGAGTG). The [α-^{32}P]dCTP (Amersham) labeled probes were generated by first-strand cDNA synthesis from total RNA isolated from 10T1/2-cells pre-treated with TTA or acetone as described previously (32). The hybridised membranes were subjected to phospho-imaging (FLA 2000, Fujifilm, Düsseldorf, Germany) overnight, and exposed to X-Ray film. Image Gauge (version 3.41) was used to quantify the results from phospo-imaging.

RESULTS

TTA-treatment of 10T1/2 cells does not effect ERK enzyme activation

We previously showed that TTA attenuates the expression of c-*fos* mRNA in response to mitogenic activators (12). As several of the early steps in cell signaling involve membrane-associated factors, we studied the mitogen-mediated activation of the down-stream factor ERK in the MAPK pathway. ERK1 was fully activated in response to platelet derived growth factor -BB (PDGF-BB) treatment (**Fig. 1**), 10% FCS, or the phorbol ester TPA (results not shown) in TTA-treated cells compared with control cells, indicating that the signal-transduction pathway leading to ERK1 activation was not affected by TTA in 10T1/2 cells. The ERK1 antibody used in this study has been reported to have some cross-specificity for ERK2. The anti-ERK1 bound similar amounts of ERK1 and ERK2 when 10T1/2 cell-lysate was subjected to SDS-PAGE and subsequently immunoblotted (result not shown). When nuclear and cytosolic fractions of stimulated 10T1/2 cells were studied by immunoblotting using anti-pERK1/2, both subtypes were equally phosphorylated, but the band corresponding to p42 ERK2 was predominantly nuclear, while the band corresponding to p44 ERK1 was predominantly cytosolic (result not shown). However, immunofluorescence stud-

ies using both anti-ERK1 and anti-pERK1/2 indicated that ERK1 and ERK2 were equally translocated to the nucleus upon stimulation.

Nuclear translocation of phosphorylated ERK is inhibited in TTA-treated 10T1/2 cells

Treating cells with factors like PDGF, TPA, or 10% FBS activates the cell-signaling pathway leading to phosphorylation and subsequent nuclear translocation of ERK. This translocation step is transient and the duration of the nuclear accumulation depends on the stimuli and the cell type. Immunofluorescence confocal microscopy showed that the cellular localisation of ERK1 was identical in resting control and TTA-treated 10T1/2 cells (**Fig. 2**). However, the translocation of ERK1 into the nucleus in response to mitogenic factors was quantitatively decreased and delayed in TTA-treated cells compared with control cells. In control cells, the majority of ERK1 was transported to the nucleus within 5 min of stimulation with 1.7 μM TPA, followed by a slow decrease in the level of nuclear ERK at 10 and 15 min. In TTA-treated cells, practically no translocation could be seen after 5 min (Fig. 2), and the maximum nuclear accumulation of ERK1, which was reached 10 to 15 min after stimulation, was considerably lower than the maximum level in control cells. At most, ERK1 appeared approximately equally distributed between the cytoplasm and the nucleus in TTA-treated cells (Fig. 2). Nuclear accumulation of ERK1 was similarly delayed in TTA-treated cells in response to 10% FBS or PDGF-BB (Results not shown). These experiments were repeated using antibodies against ERK2 with comparable results as for ERK1, indicating that in 10T1/2 cells, ERK1 and ERK2 follow a similar pattern of activation, translocation, and dephosphorylation in response to mitogen factors (results not shown). By use of a monoclonal antibody against phosphorylated p44/42 ERK1/2 (pERK1/2), we demonstrated that in TTA-treated cells stimulated with FBS for 5 min, the cytoplasmic ERK was in fact in a phosphorylated state (**Fig. 3**). The latter observation was consistent with the enzyme activity results (Fig. 1). Thus, ERK was fully activated in TTA-treated cells, but the accumulation in the nucleus in response to mitogenic factors appeared strongly impaired.

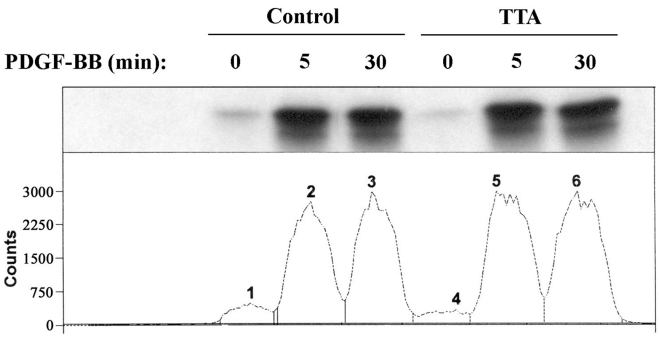

Fig. 1. Mitogen-activated protein/extracellular signal-regulated kinase (ERK) activity in tetradecylthioacetic acid (TTA)-treated versus control cells. 10T1/2 cells were grown to confluence in low-fat medium in the presence of 10 μM TTA or 10 μl acetone (control) with final medium change minimum 24 h before harvesting. Cells were stimulated with 1 unit platelet-derived growth factor-BB (PDGF-BB) for 5 or 30 min and lysed in a non-ionic detergent buffer (Materials and Methods). ERK was immunoprecipitated using rabbit polyclonal anti-ERK1, and mitogen-activated protein (MAP) kinase assay was performed as described in Materials and Methods using myelin basic protein as a substrate. Samples were subjected to SDS-PAGE and electroblotted onto a nitrocellulose membrane and radioactivity was quantified using a phospho-imager (Instant Imager, Packard Electronic Autoradiography/ Instant Imager Scanning).

TTA mediates inhibition of nuclear import, and decrease in the level of pERK1/2 dephosphorylation

In several cell lines, nuclear entry of ERK in response to mitogen factors is followed by rapid dephosphorylation and nuclear export (33). Also, it has been shown that the accumulation of ERK1/2 in the nucleus is dependent on the neosynthesis of short-lived nuclear anchoring proteins (34). Thus, the decrease in the nuclear accumulation of ERK in TTA-treated cells could be caused by an increase in the export rate, or inability to retain phosphorylated ERK in the nucleus. In control cells, phosphorylated ERK1/2 reached maximal nuclear accumulation after 5–15 min of agonist stimulation (10% FBS). After 15 to 30 min, the nuclear pERK1/2 signal started to decrease and was lost within 45 min, but pERK1/2 was still present in the cytoplasm (**Fig. 4**). Only background staining was observed 2 h after agonist treatment. In TTA-treated cells, pERK1/2 did not accumulate to the same extent in the nucleus as was the case in control cells and the staining of the pERK1/2 persisted in the cytoplasm of the agonist treated cells for more than 2 h (Fig. 4). Immunoblot analysis with anti-pERK1/2 confirmed the results from the immunofluorescence experiment (data not shown). Thus, inhibition of pERK1/2 nuclear accumulation was coupled to decreased dephosphorylation. Since, in 10T1/2 cells, nuclear ERK export was much slower than its rate of import, the low level of nuclear accumulation after agonist stimulation of TTA-treated cells were most likely due to delayed entry of ERK.

ERK in its inactive state has been shown to interact with the MAPK kinase MEK, which contains a nuclear export signal (NES) and is located in the cytoplasm (35). Upon activation, pERK disconnects from MEK and is actively transported into the nucleus as a dimer (20). In addition, it has been shown that a dimerization-deficient mutant of ERK was able to enter the nucleus, but not when fused to β-galactosidase, indicating passive diffusion of the monomeric form (21). Leptomycin B (LMB) treatment specifically blocks all nuclear export signal (NES)-mediated export by interacting irreversibly with exportin 1 (CRM1) (36, 37). This leads to nuclear accumulation of the NES-protein/nucleocytoplasmic shuttling protein MEK, and thus unphosphorylated ERK1/2 will enter the nucleus by an unknown mechanism, possibly in complex with MEK (21). After 2 h of LMB treatment, ERK1 was predominantly nuclear in control 10T1/2 cells (**Fig. 5B**). This accumulation was delayed in TTA-treated cells (Fig. 5E), further substantiating the interpretation that TTA affected and delayed nuclear import. In addition, these results

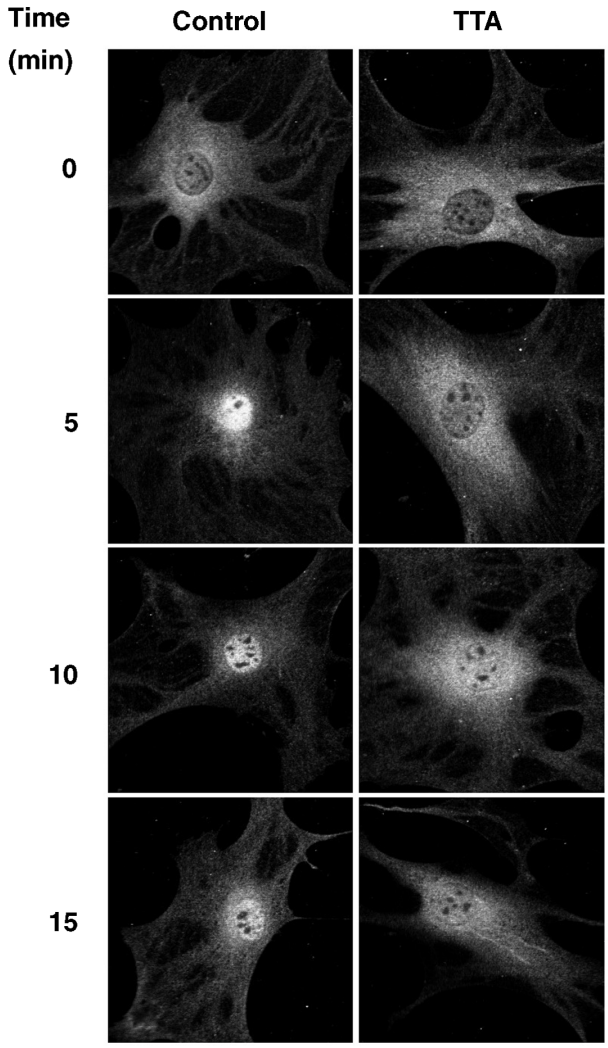

Fig. 2. Inhibition of ERK nuclear accumulation in response to 12-*O*-tetradecanoyl phorbol-13-acetate (TPA) treatment in TTA-treated cells. 10T1/2 cells grown to confluence in low-fat medium in the presence or absence of 10 μM TTA were reseeded onto coverslips and grown under the same conditions for at least 3 days to make sure no mitogenic factors remained in the cell-medium. Cells were then treated with 1.7 μM TPA for 5, 10, or 15 min, and fixed according to Materials and Methods. Cells were stained for indirect immunofluorescence using rabbit polyclonal anti-ERK1 and visualized using fluorescein (FITC)-conjugated goat-anti-rabbit antibodies. Cells were viewed through a 40× lens using confocal microscopy. The left panel shows the localisation of ERK1 in control cells while the right panel shows the localisation in TTA-treated cells. All images are from the middle layer of the cells, and are representative of at least 10 individual experiments. Images of individual cells represent the nucleocytoplasmic ERK distribution in 80–90% of the cells in a typical experiment.

showed that the delay in nuclear import was not restricted to the import of dimerized pERK2. Two hour LMB-treatment followed by 5 min stimulation with 10% FBS led to strong nuclear accumulation of ERK in control cells and a more moderate nuclear accumulation in TTA-treated cells (Fig. 5C, F). With prolonged LMB treatment total nuclear accumulation of ERK could be obtained in TTA-treated cells.

TTA generates changes in nuclear membrane fatty acid composition

The fatty acid composition of the nuclear membrane was determined (**Table 1**). The analysis demonstrated a high content of TTA (43%), confirming previous findings that CoA-esters of TTA is located in the nucleus (38). As a consequence, the total mole percent of saturated fatty acid increased in TTA-treated versus control cells. The total mol% of unsaturated fatty acid was decreased about 50% in TTA-treated cells, resulting in an increased ratio of saturated/unsaturated fatty acids and decreased double bond index (DBI). A small but significant amount of Δ^9-desaturated TTA was found in the nuclear membrane fraction (Table 1). The percentage of total polyunsaturated fatty acids was slightly increased in TTA-treated cells. This was consistent in both n-6 and n-3 series, as well as in individual long chained polyunsaturated fatty acids. Table 1 also shows the fatty acid composition in the post-nuclear membrane fraction of TTA-treated 10T1/2 cells. This cellular fraction also contained high level of TTA, but the ratio of saturated fatty acids to monounsaturated fatty acids was not as dramatically changed as seen in the nuclear membrane fraction. In contrast to the nuclear membrane, the ratio of 18:1n-9/18:0 was increased in cellular membranes of TTA-treated cells, indicating that Δ^9-desaturase activity was increased by addition of TTA. The ratio of 16:1n-7/16:0 was also increased 2-fold in both nuclear and the post-nuclear fraction. Moreover, the double bond in-

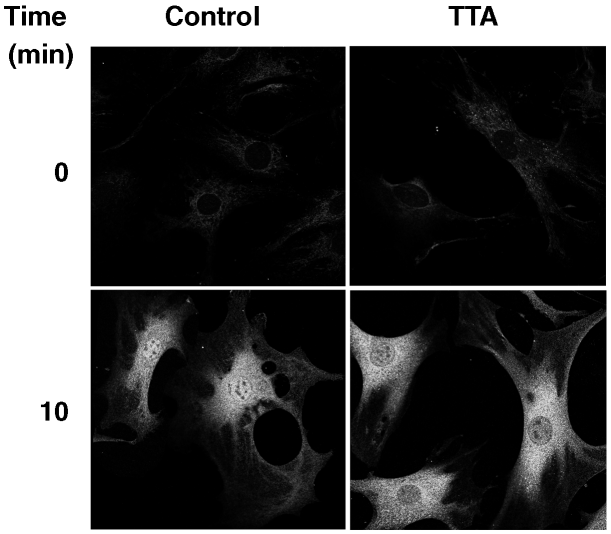

Fig. 3. Activated ERK is excluded from the nucleus of TTA-treated cells. 10T1/2 cells grown in the presence or absence of TTA were treated with 10% FBS for 10 min and subjected to indirect immunofluorescence using a monoclonal antibody to p44/42 ERK1/2 combined with Biotin-conjugated goat-anti-mouse antibodies followed by FITC-streptavidine. Cells were viewed thorough a 40× lens and images were collected from the middle sections of the cells using confocal microscopy. The left panel shows the localisation of p44/42 ERK1/2 in control cells while the right panel shows the localisation in TTA-treated cells. The images of untreated cells show background staining. All images are representative of at least three individual experiments.

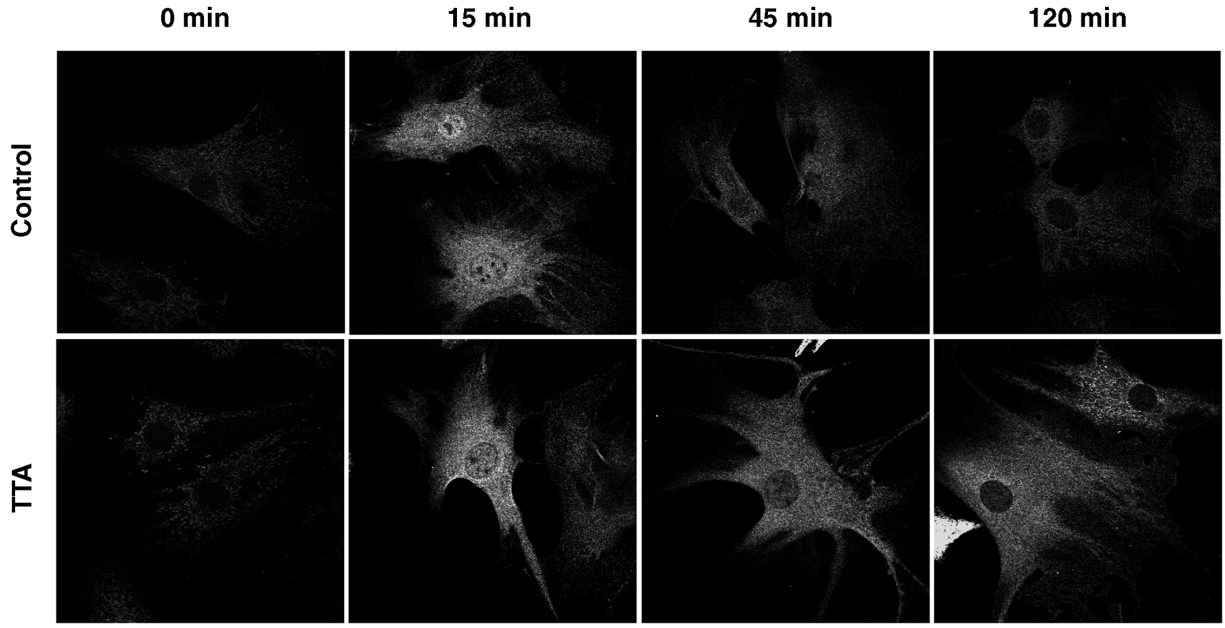

Fig. 4. Dephosphorylation of ERK1/2 is inhibited in TTA-treated cells. 10T1/2 cells were grown in the presence or absence of TTA, incubated with 10% FBS for 0 min, 15 min, 45 min or 2 h, and fixed as described in Materials and Methods and in legends to Fig. 2. The localisation of ERK was visualized using anti-p44/42 ERK1/2 antibodies combined with biotin-conjugated anti-mouse antibodies followed by FITC-streptavidin. Images were viewed through a 40× lens and collected from the middle section of the cells using confocal microscopy. The upper panel shows the localisation of p44/42 ERK1/2 in control cells while the lower panel shows the localisation in TTA-treated cells.

dex indicates that the relative increase in saturation was higher in nuclear than in post-nuclear membranes.

Nuclear translocation of PKCα and β1 was inhibited in TTA-treated cells

We have previously shown that, in contrast to PDGF-BB, TPA generates a major rearrangement of PKCα and β_1 in 10T1/2 cells, including translocation into the nucleus (25). We now show that treatment of cells with 10% FBS also generated nuclear translocation of PKCβ_1 (**Fig. 6**) and PKCα (Results not shown). We used this observation to examined whether the inhibition of entry into the nucleus was specific for ERK, or if other proteins traversing the nuclear membrane were affected by TTA. Nuclear translocation of PKCα and β_1 in response to TPA or serum was delayed in TTA-treated cells (Fig. 6), demonstrating that the inhibition of entry into the nucleus is a feature affecting other signal pathway proteins in addition to ERK. Treatment of 10T1/2 cells with the cytoskeleton-disrupting agent colchicine showed that nuclear translocation of PKCβ_1 and ERK1/2 depended on an intact cytoskeleton (results not shown). We also studied the translocation of the signal transduction proteins Abl, Stat1, and Stat5a since they are known to enter the nucleus upon stimulation in several cell lines. However, in 10T1/2 cells these proteins did not show any major rearrangement in response to the different mitogenic factors used (results not shown).

TTA has a differential effect on protein translocation across the nuclear membrane

The pathways of the proteins studied so far have not been completely elucidated, and neither ERK1/2 nor PKCα and β_1 contain a known NLS. To study the import of a protein with a classical NLS, an in vitro semi-intact cell free assay was used (31). The NLS from SV40 large T antigen was chemically fused to BSA together with the flu-

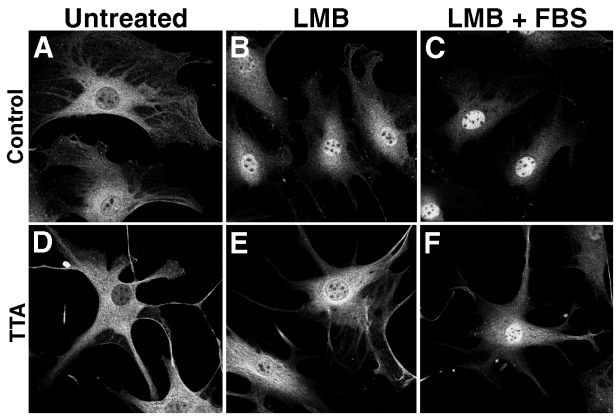

Fig. 5. Unphosphorylated ERK enters the nucleus when cells are subjected to LMB, and this nuclear accumulation is delayed in TTA-treated cells. 10T1/2 cells grown in the presence or absence of TTA were subjected to 2 h treatment with 3 nM LMB prior to stimulation, fixation, and immunological staining as described in legends to Fig. 2 and in Materials and Methods. The localisation of ERK was visualized using anti-ERK1 antibodies combined with FITC-conjugated anti-rabbit antibodies. Images were viewed through a 40× lens and collected from the middle section of the cells using confocal microscopy. The upper panel shows the localisation of ERK in control cells while the lower panel shows ERK localisation in TTA-treated cells. A and D show untreated cells, B and E show cells treated with LMB for 2 h, and C and F show cells treated with LMB for 2 h with 10% FBS included in the last 5 min. All images are representative of at least 3 individual experiments.

TABLE 1. Fatty acid composition (mol% of total fatty acids) of nuclear and cell membranes of control and TTA-treated cells

	Nuclear Membranes		Cell Membranes	
Acids	Control	TTA	Control	TTA
C14:0	1.43	0.53	1.49	0.91
C16:0	18.54	7.68	21.59	10.42
C16:1n-9	3.50	0.75	2.55	0.88
C16:1n-7	3.37	2.32	2.24	2.14
C18:0	13.57	7.33	17.52	9.35
C18:1n-9	24.62	13.20	19.79	13.65
C18:1n-7	9.05	2.85	6.53	2.76
C18:2n-6	0.73	1.09	0.61	1.12
C18:3n-6	0.04	0.05	0.06	0.07
C18:3n-3	0.02	0.04	0.07	0.11
C20:1n-9	0.60	0.15	0.56	0.21
C20:3n-9	4.95	0.79	4.53	0.94
C20:3n-6	0.50	0.65	0.50	0.66
TTA	—	42.79	—	35.51
C20:4n-6	5.27	5.81	4.90	5.01
TTA:1n-8	—	3.67	—	3.35
C20:5n-3	0.62	0.79	0.63	0.72
C24:0	0.70	0.41	1.43	0.83
C22:4n-6	0.81	0.69	0.84	0.76
C24:1n-9	1.42	0.52	2.58	0.94
C22:5n-3	2.67	2.79	2.75	3.02
C22:6n-3	3.17	3.27	3.28	3.30
Minor FA	4.42	1.84	5.56	3.36
SFA	35.59	59.38	44.74	58.80
MUFA	45.48	24.48	36.83	25.30
PUFAn-6	7.50	8.47	7.18	7.83
PUFAn-3	6.48	6.89	6.73	7.15
PUFA	13.98	15.36	13.91	14.98
SFA/MUFA	0.78	2.43	1.21	2.32
SFA/PUFA	2.55	3.87	3.22	3.93
SFA-TTA/MUFA-TTA	10.78	0.80	1.21	1.06
PUFAn-3/PUFAn-6	0.86	0.81	0.94	0.91
18:1n-9/18:0	1.81	1.80	1.13	1.46
16:1n-7/16:0	0.18	0.30	0.10	0.21
DBI	1.24	0.96	1.14	0.95

Abbreviations: DBI, double bond index (the sum of the percentage of each fatty acid multiplied by the number of double bonds in that fatty acid divided by 100); Minor FA, the sum of C12:0, C15:0 C17:0, C17:1n-8, C20:0, C20:1n-11, C20:1n-7, C20:2n-6, C22:0, C22:1n-9, and C22:5n-6; MUFA, total monounsaturated fatty acids; MUFA-TTA:1, total monounsaturated fatty acids without TTA:1n-8; PUFA, total polyunsaturated fatty acids; SFA, total saturated fatty acids; SFA-TTA, total saturated fatty acids without TTA; TTA, tetradecylthioacetic acid; C16:0iso, C17:0anteiso.

orescent marker FITC, and delivered to digitonin permeabilized cells. When supplemented with reticulocyte lysate, NLS-BSA-FITC was rapidly imported to the nucleus both in control cells (**Fig. 7**, upper panel) and in TTA-treated cells (Fig. 7, lower panel), demonstrating exclusively nuclear localization after 30 min of incubation. When the permeabilized cells were incubated with NLS-BSA-FITC without reticulocyte lysate, no import could be seen after 30 min (Fig. 7). Thus, the import of BSA fused to a classical NLS did not show any detectable inhibition in TTA-treated versus control cells. As expected, a complex of FITC-BSA or FITC-BSA fused to the nuclear export signal (NES) from the HIV-1 protein Rev, did not enter the nucleus (result not shown).

In addition, we studied the nuclear import of the endogenous NLS-containing protein hnRNP A1 (**Fig. 8**). The pre-mRNA binding protein hnRNP A1 shuttles continuously in and out of the nucleus (39), but is predominantly localized to the nucleoplasm (Fig. 8A, D). In order to study its nuclear import, we treated 10T1/2 cells with Actinomycin D, which gave a mixed cytoplasmic and nuclear localisation of hnRNP A1 in the treated cells (Fig. 8B, E). In 2–5% of the cells, the cytoplasmic signal was strong and these cells were used to determine the effect of TTA on hnRNP A1 translocation. When Actinomycin D was removed, RNA synthesis and thus the nuclear localization of hnRNP A1 was recovered (40), so that after 20 min a 30% decrease in cells with strong cytoplasmic staining was seen (not shown), and after 1 h no strong cytoplasmic staining remained (Fig. 8C, F). Cell-fractionation and subsequent SDS-PAGE and immunoblotting supported the results from the immunofluorescence experiment (not shown). Thus, as demonstrated in Fig. 8, and consistent with the in vitro results (Fig. 7), TTA-treatment had no evident effect on the import kinetics of the classical NLS-containing protein hnRNP A1.

The expression of mRNAs encoding proteins involved in nuclear import is not affected by TTA-treatment

It has previously been shown that TTA affects the level of expression of genes involved in the fatty acid metabolism (6, 8, 10, 11). Therefore, the possibility of a TTA-mediated down-regulation of proteins important for transport across the nuclear membrane had to be investigated. Dot-blot analysis was carried out to analyze the level of RNA expression of the import factors Importin α, Importin β, Importin 7, and nuclear transport factor 2 (NTF2). DNA fragments acquired by PCR of cDNA from 10T1/2 cells using specific primers for *importin α*, *importin β*, *importin 7,* and *NTF2* were dotted on the membranes, with *actin* as the reference gene (**Fig. 9**). Hybridization reactions were carried out using a ^{32}P-labeled first-strand cDNA probe prepared from RNA purified from 10T1/2 cells with/without TTA-pre-treatment. Quantification of the results showed no significant variations in the relative expression level of the studied import factors in TTA-treated versus control cells (Fig. 9). In addition, cDNA from 10T1/2 cells with/without TTA-pre-treatment was subjected to semi-quantitative PCR using a combination of the primers for the *actin* gene and the genes of the different import factors. The results obtained by semi-quantitative PCR confirmed the Dot-blot analysis (result not shown).

DISCUSSION

The thia-fatty acid TTA causes a marked decrease in TPA and PDGF-BB induced c-*fos* mRNA expression. We have earlier shown that TTA has a prominent effect on phospholipid metabolism in 10T1/2 cells by increasing the incorporation of inorganic phosphate into glycerophospholipids, particularly phosphatidyletanolamine (4). TTA-containing glycerophospholipids are slightly more hydrophilic than glycerophospholipids containing natural acyl groups (2). The dominating finding in the present

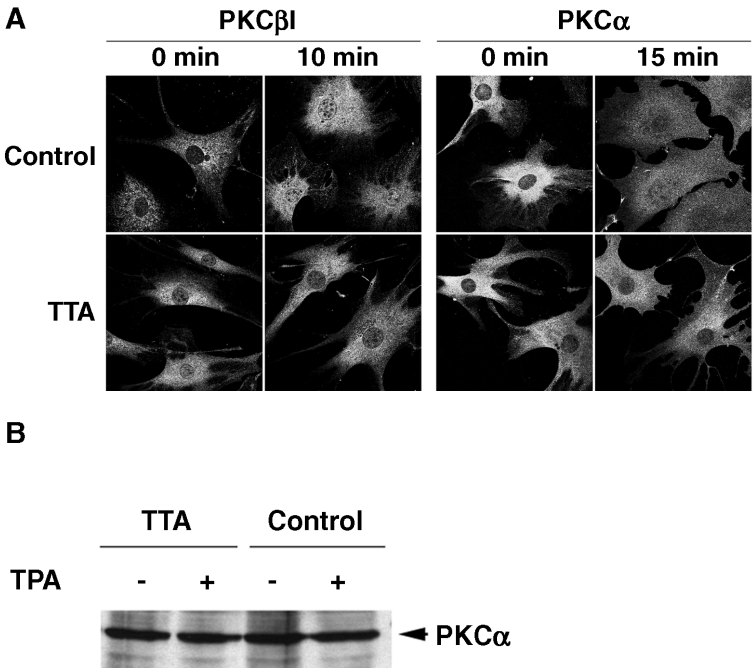

Fig. 6. The nuclear translocation of protein kinase C (PKC)α and PKCβ_1 in response to FBS is inhibited in TTA-treated 10T1/2 cells. A: 10T1/2 cells were grown in the presence or absence of TTA. For studies of PKCβ_1 translocation, cells were incubated with 10% FBS for 10 min, and for studies of PKCα translocation, cells were incubated with 1.7 μM TPA for 15 min. Cells were fixed as described in Materials and Methods. The localisation of PKCβ_1 was visualized using anti-PKCβ_1 antibodies, and the localisation of PKCα was visualized using anti-PKCα antibodies, both combined with FITC-conjugated anti-rabbit antibodies. Images were viewed through a 40× lens and collected from the middle section of the cells using confocal microscopy. B: The total amount of PKCα was determined by immunoblot analysis. Cells with or without TTA in the medium were grown to confluence with final medium change 24 h prior to harvesting. The cells were incubated with 1.7 μM TPA and lysed. About 20 μg of protein was separated on 10% SDS-PAGE gels and subsequently blotted onto nitrocellulose membranes. Membranes were incubated with rabbit polyclonal antibodies against c-PKCα (1:500, v/v). Bound antibodies were visualized using HRP-conjugated anti-rabbit IgG followed by enhanced chemoluminiscence (ECL) detection using X-Ray film.

study regarding the fatty acid composition was the overall decrease in monounsaturated fatty acids after TTA treatment. The latter may be biologically important, particularly the substantial decrease in oleic acid (C18:1n-9). The predominant incorporation of TTA into membrane lipids may be due to its slow oxidation rate relative to naturally occurring monounsaturated fatty acids (41). This change in fatty acid composition is indicative of a more rigid membrane since oleic acid is known to favor the hexagonal over the lamellar structure of membranes (42). In addition, TTA is believed to have saturated fatty acid properties and, therefore, substituting TTA for oleic acid or

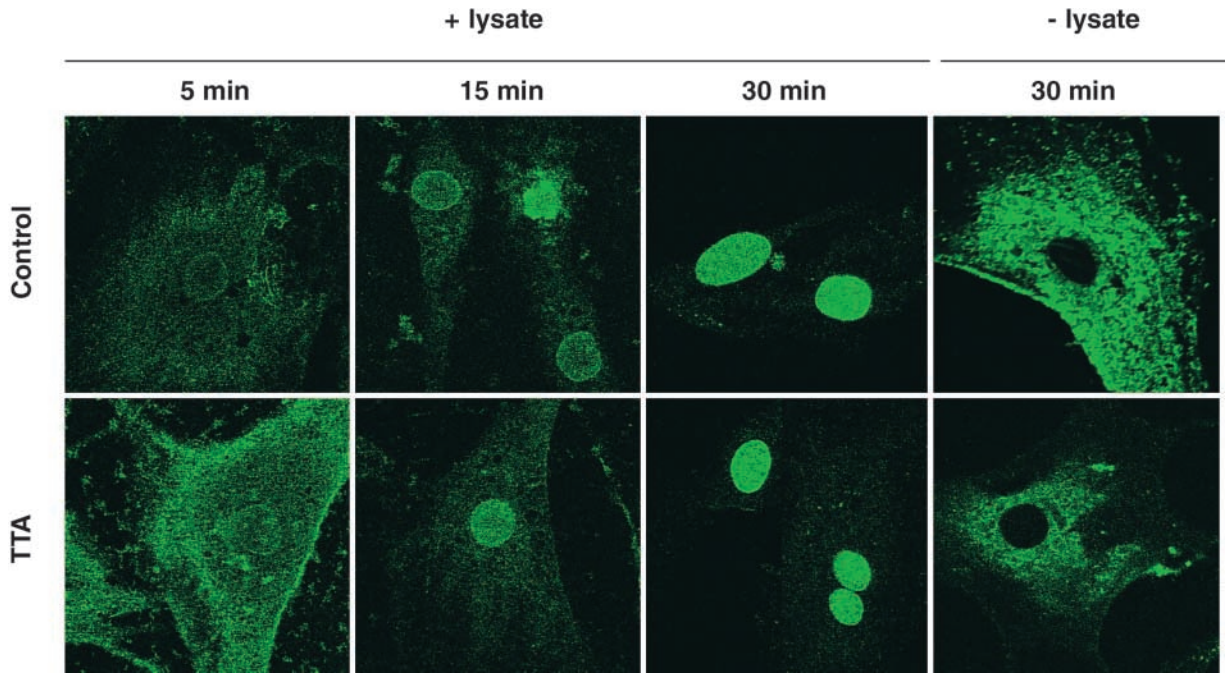

Fig. 7. Nuclear import of nuclear localization signal (NLS)-BSA-FITC is not inhibited in permeabilized TTA-treated cells compared with control cells. Prior to the in vitro semi intact cell free assay, 10T1/2 cells were grown in the presence or absence of TTA and reseeded on glass-coverslips. Twenty-four hours later, digitonin-permeabilization was performed as described in Materials and Methods. Permeabilized cells were then incubated for 5, 15, or 30 min with the NLS from SV40 large T fused to BSA-FITC in the presence of ATP and reticulocyte lysate. In addition, cells were incubated for 30 min with NLS-BSA-FITC and ATP without reticulocyte lysate present. Cells were then fixed and mounted, as described in the Immunofluorescence procedure. Images were viewed through a 40× lens and collected from the middle section of the cells using confocal microscopy.

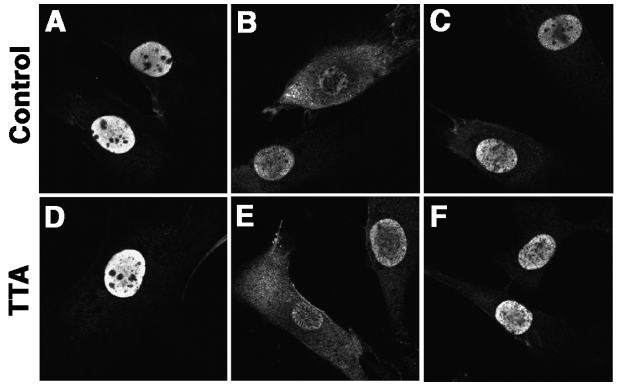

Fig. 8. Nuclear import of hnRNP A1 in 10T1/2 cells after treatment with Actinomycin D. Cells with or without TTA were seeded onto coverslips and treated with 10 μg/ml cycloheximide (A and D) or 10 μg/ml cycloheximide and 10 μg/ml Actinomycin D (B, C, E, F) for 3 h. The medium was then removed and the cells washed once with conditioned cell-medium after which conditioned cell-medium containing cycloheximide was added. Incubation was continued for 1 h (C and F). Cells were fixed and immunofluorescence was performed as described in Materials and Methods using the monoclonal antibody 4B10 combined with FITC-conjugated goat-anti-mouse IgG. The number of cells showing translocation of hnRNP A1 from the nucleoplasm to the cytoplasm was determined. Images were viewed through a 63× lens and collected from the middle section of the cells using confocal microscopy.

other unsaturated fatty acids, would favor the more rigid lamellar structure. Taken together, the present data and the previous finding that some PE species increase in TTA-treated cells indicate that the TTA-effect may be lipid species specific.

There were many potential candidate steps where the PDGF-mediated signal transduction pathway leading to c-*fos* expression could be disrupted by TTA. Previous experiments have shown that TTA can be incorporated into the second messenger diacylglycerol (DAG) (S. A. Eiane, C. Helleland, R. K. Berge, J. R. Lillehaug, and H. Holmsen, personal communication), and thereby create a DAG that activates PKC poorly. If this was the most prominent effect of TTA, the TPA-induced signal transduction pathway would not be affected since TPA mimics, and replaces, DAG in activating PKC directly (43). The attenuation of TPA-mediated c-*fos* mRNA expression in TTA-treated cells (12) argues against a DAG effect and suggests that TTA might alter lipid and/or membrane composition important for PKC mediated signal transduction downstream of DAG synthesis.

MAPK assays showed that ERK was fully activated after TPA and PDGF-BB stimulation in both TTA-treated cells and control-cells (Fig. 1). These results suggest that TTA does not affect the signal transduction pathway upstream of ERK. Considering that ERK needs to pass through the nuclear membrane pores in order to phosphorylate and activate nuclear factors, alterations in the nuclear membrane structure could affect pore function and thus ERK translocation. We found a marked decrease in the translocation of phosphorylated ERK1/2 in TTA-treated cells compared with control cells (Figs. 2 and 3). There did not seem to be any difference in the activation pattern of ERK1 and ERK2, nor in the susceptibility to the TTA-caused inhibition of import. Thus, our results indicate that treating the cells with a non-β-oxidable fatty acid markedly attenuates the ERK1/2 nuclear accumulation through an unknown mechanism, which could explain the inhibition of c-*fos* expression. TTA generates dramatic changes in the membrane ratio of saturated to monounsaturated fatty acids, especially in the nuclear membrane, and this may affect pore function. Lipid modification may play an important role in the membrane association of the cytoskeleton and it is known that about one third of ERK is associated with the microtubule cytoskeleton (44). Immunofluorescence studies of Actin and β-tubulin architecture showed no major differences in control cells and TTA-treated cells (result not shown). We can, however, not conclude that the cytoskeleton in TTA-treated cells is not altered, but it may be altered in a manner we cannot observe with the techniques we have used.

To see whether TTA inhibited the nuclear import of ERK1/2, or affected their export, we treated the cells with Leptomycin B (Fig. 5). The relocalisation of dephosphorylated ERK from the nucleus to the cytoplasm is coupled to the export of MEK (33), which contains a nuclear export signal (NES) (45). Thus, no export of ERK will take place when the NES-pathway is blocked. In the presence of LMB, a distinctive slower nuclear accumulation of ERK1/2 could be seen in TTA-treated cells compared with control cells. Since the entry of ERK in response to LMB most likely takes place as a MEK-ERK complex (21), and probably uses a different pathway from the dimeriza-

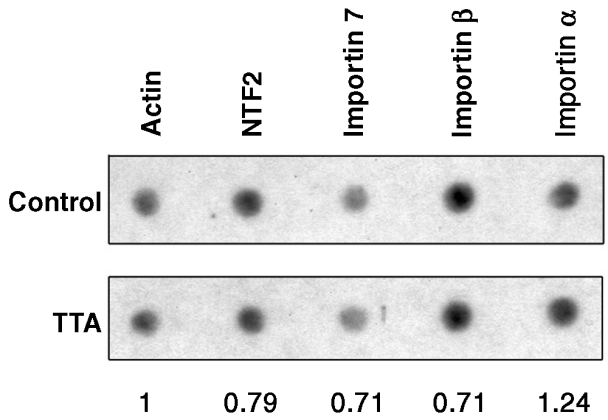

Fig. 9. The mRNA-expression of Importin α, Importin β, Importin 7, and NTF2 was assayed by hybridisation using complex cDNA probes. DNA fragments from the different genes were generated as described in Materials and Methods and applied on HybondN+ membranes. Actin was used as reference gene. The probes were generated by first-strand cDNA synthesis of total RNA from control (top panel) or TTA-treated (lower panel) 10T1/2-cells. Each hybridization mixture contained approximately 10^6 cpm. per 1 ml (Materials and Methods). The ratio of the relative values of the TTA-hybridisation signal and the control-hybridisation signal is given below each sample, and are based on two individual experiments. Image Gauge V 3.41 software was used for the quantification of the hybridisation results.

tion-dependent pERK1/2 pathway, the LMB results are consistent with a nuclear import of ERK through different pathways, inhibited by TTA. However, with prolonged LMB treatment, total nuclear accumulation of ERK was obtained in TTA-treated cells. We also showed that dephosphorylation of ERK was delayed in TTA-treated cells compared with control cells, indicating a slower level of dephosphorylation when ERK had decreased access to the nuclear compartment. The main part of ERK1/2 dephosphorylation takes place in the nucleus (46), and our results are consistent with this.

Our results show that in addition to ERK, TTA significantly inhibits the nuclear import of PKCα and PKCβ_1. The mechanisms for ERK1/2 nuclear import appear to share some common features with PKCα and PKCβ_1 nuclear import since they are all cytoskeleton dependent (results not shown, 47, 48). In comparison, it has been shown that the import of BSA coupled to a canonical NLS is not cytoskeleton dependent (47). There are indications that the import mechanism of PKCs does not follow the usual NLS-guided pathway, since Schmalz et al. (49) have shown that the nuclear translocation of PKCα is not linked to the classical import factors Importin β and RanGTP. However, there is an energy-dependent step, and the rate of the nuclear translocation, as well as the size of the proteins, are arguments for an active translocation mechanism and against uptake by free diffusion (49). In contrast, ERK import seems to be dependent on both Importin β and RanGTP, shown by use of the inhibitors wheat germ agglutinin and RanQ69L (21). Also, a homolog of ERK in *Drosophila*, D-ERK, has been linked to import factors DIM-7 and Ketel, homologs of vertebrate Importin 7 and Importin β, respectively (50). Consistent with these findings is the possibility that ERK may be imported through the direct interaction with the NPC (22, 23). If this latter mechanism is active, then changes in membrane lipid composition may cause alterations to the NPC thereby inhibiting nuclear ERK import.

In the present report, we demonstrate that TTA-treatment affect the import of two classes of proteins known to use different nuclear import pathways. Thus, our data indicate that the inhibition of nuclear translocation is not restricted to one transport pathway, but is rather related to a more general perturbation of the nuclear import machinery. However, the in vitro nuclear import of a reporter protein linked to the canonical NLS sequence from SV40 large T antigen, and the in vivo import of the NLS (M9)-containing protein hnRNP A1, was not inhibited in TTA-treated cells (Fig. 8). As proteins containing a NLS use classical import pathways, which are different from the pathways used by the PKs studied here, TTA may have a differential effect depending on the nature and/or strength of the import signal and on the factors involved in the import through the NPC. Since the gene expression of four essential transport factors was not affected by TTA-treatment (Fig. 9), we hypothesize that TTA replaces naturally occurring monounsaturated fatty acids, especially oleic acid, producing more lamellar, and rigid, nuclear membrane structures perturbing efficient transport through the NPC of proteins lacking classical NLS, thereby affecting negatively signal transduction. Detailed studies of nuclear pore structure and function in cells treated with TTA will be needed to elucidate these mechanisms further.

The authors wish to thank Mrs. H. Kanestrøm and Ms. I. Hageberg for their devoted technical assistance. The project is supported by grants from the Norwegian Cancer Society (B.B. and C.H.); the Norwegian Research Council; and the Locus on Cancer Research, the Faculty of Medicine, University of Bergen.

REFERENCES

1. Berge, R. K., and E. Hvattum. 1994. Impact of cytochrome P450 system on lipoprotein metabolism. Effect of abnormal fatty acids (3-thia fatty acids). *Pharmacol. Ther.* **61:** 345–383.
2. Skrede, S., H. N. Sorensen, L. N. Larsen, H. H. Steineger, K. Hovik, O. S. Spydevold, R. Horn, and J. Bremer. 1997. Thia fatty acids, metabolism and metabolic effects. *Biochim. Biophys. Acta.* **1344:** 115–131.
3. Kryvi, H., A. Aarsland, and R. K. Berge. 1990. Morphologic effects of sulfur-substituted fatty acids on rat hepatocytes with special reference to proliferation of peroxisomes and mitochondria. *J. Struct. Biol.* **103:** 257–265.
4. Skorve, J., D. Asiedu, A. C. Rustan, C. A. Drevon, A. al Shurbaji, and R. K. Berge. 1990. Regulation of fatty acid oxidation and triglyceride and phospholipid metabolism by hypolipidemic sulfur-substituted fatty acid analogues. *J. Lipid Res.* **31:** 1627–1635.
5. Aarsland, A., and R. K. Berge. 1991. Peroxisome proliferating sulphur- and oxy-substituted fatty acid analogues are activated to acyl coenzyme A thioesters. *Biochem. Pharmacol.* **41:** 53–61.
6. Raspe, E., L. Madsen, A. M. Lefebvre, I. Leitersdorf, L. Gelman, J. Peinado Onsurbe, J. Dallongeville, J. C. Fruchart, R. Berge, and B. Staels. 1999. Modulation of rat liver apolipoprotein gene expression and serum lipid levels by tetradecylthioacetic acid (TTA) via PPARalpha activation. *J. Lipid Res.* **40:** 2099–2110.
7. Asiedu, D. K., A. al Shurbaji, A. C. Rustan, I. Bjorkhem, L. Berglund, and R. K. Berge. 1995. Hepatic fatty acid metabolism as a determinant of plasma and liver triacylglycerol levels. Studies on tetradecylthioacetic and tetradecylthiopropionic acids. *Eur. J. Biochem.* **227:** 715–722.
8. Demoz, A., H. Vaagenes, N. Aarsaether, E. Hvattum, J. Skorve, M. Gottlicher, J. R. Lillehaug, G. G. Gibson, J. A. Gustafsson, and S. Hood. 1994. Coordinate induction of hepatic fatty acyl-CoA oxidase and P4504A1 in rat after activation of the peroxisome proliferator-activated receptor (PPAR) by sulphur-substituted fatty acid analogues. *Xenobiotica.* **24:** 943–956.
9. Madsen, L., A. Garras, G. Asins, D. Serra, F. G. Hegardt, and R. K. Berge. 1999. Mitochondrial 3-hydroxy-3-methylglutaryl coenzyme A synthase and carnitine palmitoyltransferase II as potential control sites for ketogenesis during mitochondrion and peroxisome proliferation. *Biochem. Pharmacol.* **57:** 1011–1019.
10. Madsen, L., and R. K. Berge. 1999. 3-Thia fatty acid treatment, in contrast to eicosapentaenoic acid and starvation, induces gene expression of carnitine palmitoyltransferase-II in rat liver. *Lipids.* **34:** 447–456.
11. Vaagenes, H., L. Madsen, D. K. Asiedu, J. R. Lillehaug, and R. K. Berge. 1998. Early modulation of genes encoding peroxisomal and mitochondrial beta- oxidation enzymes by 3-thia fatty acids. *Biochem. Pharmacol.* **56:** 1571–1582.
12. Helleland, C., S. A. Eiane, R. K. Berge, H. Holmsen, and J. R. Lillehaug. 1997. 1-(Carboxymethylthio)tetradecane attenuates PDGF- and TPA-induced c-fos mRNA expression and increases the formation of phosphatidylethanolamine with a shift from less to more polar molecular species in C3H/10T1/2 cells. *Exp. Cell Res.* **236:** 330–340.
13. Chen, R. H., C. Sarnecki, and J. Blenis. 1992. Nuclear localization and regulation of erk- and rsk-encoded protein kinases. *Mol. Cell. Biol.* **12:** 915–927.
14. Gonzalez, F. A., A. Seth, D. L. Raden, D. S. Bowman, F. S. Fay, and

R. J. Davis. 1993. Serum-induced translocation of mitogen-activated protein kinase to the cell surface ruffling membrane and the nucleus. *J. Cell Biol.* **122:** 1089–1101.
15. Lenormand, P., C. Sardet, G. Pages, G. L'Allemain, A. Brunet, and J. Pouyssegur. 1993. Growth factors induce nuclear translocation of MAP kinases (p42mapk and p44mapk) but not of their activator MAP kinase kinase (p45mapkk) in fibroblasts. *J. Cell Biol.* **122:** 1079–1088.
16. Hill, C. S., R. Marais, S. John, J. Wynne, S. Dalton, and R. Treisman. 1993. Functional analysis of a growth factor-responsive transcription factor complex. *Cell.* **73:** 395–406.
17. Brunet, A., D. Roux, P. Lenormand, S. Dowd, S. Keyse, and J. Pouyssegur. 1999. Nuclear translocation of p42/p44 mitogen-activated protein kinase is required for growth factor-induced gene expression and cell cycle entry. *EMBO J.* **18:** 664–674.
18. Fukuda, M., Y. Gotoh, and E. Nishida. 1997. Interaction of MAP kinase with MAP kinase kinase: its possible role in the control of nucleocytoplasmic transport of MAP kinase. *EMBO J.* **16:** 1901–1908.
19. Blanco-Aparicio, C., J. Torres, and R. Pulido. 1999. A novel regulatory mechanism of MAP kinases activation and nuclear translocation mediated by PKA and the PTP-SL tyrosine phosphatase. *J. Cell Biol.* **147:** 1129–1136.
20. Khokhlatchev, A. V., B. Canagarajah, J. Wilsbacher, M. Robinson, M. Atkinson, E. Goldsmith, and M. H. Cobb. 1998. Phosphorylation of the MAP kinase ERK2 promotes its homodimerization and nuclear translocation. *Cell.* **93:** 605–615.
21. Adachi, M., M. Fukuda, and E. Nishida. 1999. Two co-existing mechanisms for nuclear import of MAP kinase: passive diffusion of a monomer and active transport of a dimer. *EMBO J.* **18:** 5347–5358.
22. Matsubayashi, Y., M. Fukuda, and E. Nishida. 2001. Evidence for existence of a nuclear pore complex-mediated, cytosol-independent pathway of nuclear translocation of ERK MAP Kinase in permeabilized cells. *J. Biol. Chem.* **276:** 41755–41760.
23. Whitehurst, A. W., J. L. Wilsbacher, Y. You, K. Luby-Phelps, M. S. Moore, and M. H. Cobb. 2002. ERK2 enters the nucleus by a carrier-independent mechanism. *Proc. Natl. Acad. Sci. USA.* **99:** 7496–7501.
24. Meili, R., and K. Ballmer-Hofer. 1996. Activation-independent nuclear translocation of mitogen activated protein kinase ERK1 mediated by thiol-modifying chemicals. *FEBS Lett.* **394:** 34–38.
25. Bjørndal, B., C. Helleland, and J. R. Lillehaug. 2000. Differential TPA and PDGF-BB effects on subcellular localisation of PKC alpha and beta I in C3H/10T1/2 cells. *Anticancer Res.* **20:** 2633–2640.
26. Male, R., J. R. Lillehaug, R. Djurhuus, and I. F. Pryme. 1985. In vitro transformation and tumor promotion studies of styrene and styrene oxide. *Carcinogenesis.* **6:** 1367–1370.
27. Blight, E. G., and M. J. Dyer. 1959. A rapid method of total lipid extraction and purification. *J. Biochem. Physiol.* **37:** 911–917.
28. Morrison, W. R., and L. M. Smith. 1964. Preparation of fatty acid methyl esters and dimethylacetals from lipids with boron fluoride-methanol. *J. Lipid Res.* **5:** 600–608.
29. Kates, M. 1986. General analytical procedures. *In* Techniques in Lipidology. M. Dates, editor. Elsevier Science Publishers, Amsterdam. 112–185.
30. Bohov, P., V. Balaz, and J. Hrivnak. 1984. Analysis of fatty acid methyl esters on an SP 2340 glass capillary column. *J. Chromatogr.* **286:** 247–257.
31. Hassel, I., V. Cezanne, C. Trevino, H. Schlatter, I. Romero Matuschek, A. Schmidt, and H. Fasold. 1996. Export of ribosomal subunits from resealed rat liver nuclear envelopes. *Eur. J. Biochem.*. **241:** 32–37.
32. Fluge, O., D. R. Haugen, L. A. Akslen, A. Marstad, M. Santoro, A. Fusco, J. E. Varhaug, and J. R. Lillehaug. 2001. Expression and alternative splicing of c-ret RNA in papillary thyroid carcinomas. *Oncogene.* **20:** 885–892.
33. Adachi, M., M. Fukuda, and E. Nishida. 2000. Nuclear export of MAP kinase (ERK) involves a MAP kinase kinase (MEK)- dependent active transport mechanism. *J. Cell Biol.* **148:** 849–856.
34. Lenormand, P., J. M. Brondello, A. Brunet, and J. Pouyssegur. 1998. Growth factor-induced p42/p44 MAPK nuclear translocation and retention requires both MAPK activation and neosynthesis of nuclear anchoring proteins. *J. Cell Biol.* **142:** 625–633.
35. Tolwinski, N. S., P. S. Shapiro, S. Goueli, and N. G. Ahn. 1999. Nuclear localization of mitogen-activated protein kinase kinase 1 (MKK1) is promoted by serum stimulation and G2-M progression. Requirement for phosphorylation at the activation lip and signaling downstream of MKK. *J. Biol. Chem.* **274:** 6168–6174.
36. Fukuda, M., S. Asano, T. Nakamura, M. Adachi, M. Yoshida, M. Yanagida, and E. Nishida. 1997. CRM1 is responsible for intracellular transport mediated by the nuclear export signal. *Nature.* **390:** 308–311.
37. Wolff, B., J. J. Sanglier, and Y. Wang. 1997. Leptomycin B is an inhibitor of nuclear export: inhibition of nucleo- cytoplasmic translocation of the human immunodeficiency virus type 1 (HIV-1) Rev protein and Rev-dependent mRNA. *Chem. Biol.* **4:** 139–147.
38. Elholm, M., A. Garras, S. Neve, D. Tornehave, T. B. Lund, J. Skorve, T. Flatmark, K. Kristiansen, and R. K. Berge. 2000. Long-chain acyl-CoA esters and acyl-CoA binding protein are present in the nucleus of rat liver cells. *J. Lipid Res.* **41:** 538–545.
39. Pinol-Roma, S., and G. Dreyfuss. 1992. Shuttling of pre-mRNA binding proteins between nucleus and cytoplasm. *Nature.* **355:** 730–732.
40. Vautier, D., P. Chesne, C. Cunha, A. Calado, J. P. Renard, and M. Carmo-Fonseca. 2001. Transcription-dependent nucleocytoplasmic distribution of hnRNP A1 protein in early mouse embryos. *J. Cell Sci.* **114:** 1521–1531.
41. Hvattum, E., H. J. Grav, and J. Bremer. 1993. Hormonal and substrate regulation of 3-thia fatty acid metabolism in Morris 7800 C1 hepatoma cells. *Biochem. J.* **294:** 917–921.
42. Rilfors, L., G. Lindblom, Å. Wieslander, and A. Christensson. 1984. Lipid bilayer stability in biological membranes. *In* Biomembranes, Membrane Fluidity. M. Kates and L. A. Manson, editors. Plenum Press, New York and London. 205–245.
43. Nishizuka, Y. 1984. The role of protein kinase C in cell surface signal transduction and tumour promotion. *Nature.* **308:** 693–698.
44. Reszka, A. A., R. Seger, C. D. Diltz, E. G. Krebs, and E. H. Fischer. 1995. Association of mitogen-activated protein kinase with the microtubule cytoskeleton. *Proc. Natl. Acad. Sci. USA.* **92:** 8881–8885.
45. Fukuda, M., I. Gotoh, Y. Gotoh, and E. Nishida. 1996. Cytoplasmic localization of mitogen-activated protein kinase kinase directed by its NH2-terminal, leucine-rich short amino acid sequence, which acts as a nuclear export signal. *J. Biol. Chem.* **271:** 20024–20028.
46. Todd, J. L., K. G. Tanner, and J. M. Denu. 1999. Extracellular regulated kinases (ERK) 1 and ERK2 are authentic substrates for the dual-specificity protein-tyrosine phosphatase VHR. A novel role in down-regulating the ERK pathway. *J. Biol. Chem.* **274:** 13271–13280.
47. Schmalz, D., F. Kalkbrenner, F. Hucho, and K. Buchner. 1996. Transport of protein kinase C alpha into the nucleus requires intact cytoskeleton while the transport of a protein containing a canonical nuclear localization signal does not. *J. Cell Sci.* **109:** 2401–2406.
48. Martelli, A. M., L. Cocco, R. Bareggi, G. Tabellini, R. Rizzoli, M. D. Ghibellini, and P. Narducci. 1999. Insulin-like growth factor-I-dependent stimulation of nuclear phospholipase C-beta1 activity in Swiss 3T3 cells requires an intact cytoskeleton and is paralleled by increased phosphorylation of the phospholipase. *J. Cell. Biochem.* **72:** 339–348.
49. Schmalz, D., F. Hucho, and K. Buchner. 1998. Nuclear import of protein kinase C occurs by a mechanism distinct from the mechanism used by proteins with a classical nuclear localization signal. *J. Cell Sci.* **111:** 1823–1830.
50. Lorenzen, J. A., S. E. Baker, F. Denhez, M. B. Melnick, D. L. Brower, and L. A. Perkins. 2001. Nuclear import of activated D-ERK by DIM-7, an importin family member encoded by the gene moleskin. *Development.* **128:** 1403–1414.